

Figure 2 Dependence of typical geometrical dimensions upon sintering time (PS at 180 °C).  $L$ , total length;  $D_b$ , diameter of bottom particle;  $D_t$ , diameter of top particle;  $2x$ , diameter of contact neck circle

This Figure clearly shows that with increasing time the total length decreases and the contact neck diameter increases parabolically while the particles diameters do not change appreciably over a wide range of the sintering process. This behaviour, typical of all the experiments with PS and PMMA, shows that during a significant part of the sintering period most of the changes involving viscous flow take place within and in the vicinity of the contact zone. Thus widening of the neck is at the expense of the total length with little change in shape of most of the particle. In this regard, however, it is important to point out that Frenkel, in order to maintain a constant volume model of the sharp neck corners had to assume increasing particles diameters with sintering progress.

A Frenkel-type log-log plot is shown in Figure 3 where the neck diameter is plotted against time for pairs of PS and PMMA particles. The linear dependence shown is typical of all the experiments with PS and PMMA spheres. The values of the slopes are 0.56 for PS and 0.53 for PMMA, in surprising agreement with predicted value of 0.5 from Frenkel's theory. A temperature range from 160°C to 220°C was covered for sintering of the PMMA spherical particles giving slopes of 0.49 for 160°C and 0.63 for 220°C, respectively. This slight effect of temperature on the slopes and their proximity to the predicted 0.5 value support Frenkel's Newtonian viscous flow model. This conclusion is consistent with typical sintering con-

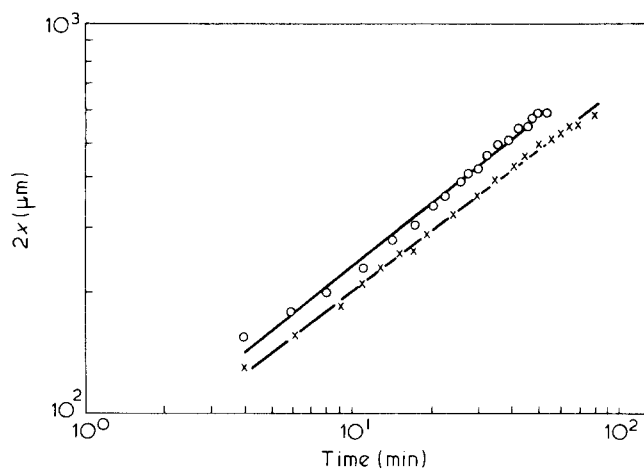


Figure 3 Linear dependence of  $\log 2x$  vs.  $\log t$ , ●, PS, 180 °C, slope = 0.56; x, PMMA, 200 °C, slope = 0.53

ditions, namely low shear rates. Interpretations in terms of a wide non-Newtonian flow behaviour and especially dilatancy can be ascribed to artefacts and not to the natural flow mechanism involved.

The sintering process for polymeric particles by coalescence is a process of highly complicated viscous flow trajectories with moving boundaries. It is thus surprising to observe good agreement between Frenkel's simplified model and the experimental results. A fundamental sintering model based upon solutions of continuity and momentum equations with proper boundary conditions is presently being developed and will be reported at later date.

#### Acknowledgement

Partial support from the Fund for the Encouragement of Research at the Technion is greatly appreciated.

#### References

- 1 Shaler, A. J. *AIME Metals Transactions* 1949, **185**, 796
- 2 Frenkel, J. J. *Phys. (USSR)* 1945, **9**, 385
- 3 Rosenzweig, N. and Narkis, M. 'A New Technique for Observation and Analysis of Polymeric Particles Undergoing Sintering', submitted for publication
- 4 Kuczynski, G. C., Neuville, B. and Toner, H. P. *J. Appl. Polym. Sci.* 1970, **14**, 2069
- 5 Narkis, M. *Polym. Eng. Sci.* 1979, **19**, 889
- 6 Lontz, J. F. 'Sintering of Polymer Materials' First Symp. on Fundamental Phenomena in the Material Sciences, Boston, Plenum, 1963

## Interpretation of radial distribution functions for non-crystalline polymers

Geoffrey R. Mitchell, Richard Lovell and Alan H. Windle

Department of Metallurgy and Materials Science, University of Cambridge, Pembroke Street, Cambridge, CB2 3QZ, UK

(Received 9 April 1980)

In investigations of the structure of non-crystalline polymers using radial distribution functions (RDFs) there has been a tendency to assume that a marked periodicity of about 5 Å extending to 20 Å and beyond is evidence of significant chain parallelism (for example see references 1

and 2). In this communication we show, first from experiment and then from model calculations, that such a periodicity is evidence only for a well defined closest distance of approach between chains.

RDFs are calculated from scattering data using the

following formula:

$$4\pi r(\rho(r) - \rho_0) = W(r) = (2/\pi) \int_0^{\infty} sZ(s) \sin rs \, ds$$

$$Z(s) = i(s)/g^2(s); \quad i(s) = kI^{corr}(s) - \sum f^2$$

$I^{corr}(s)$  is the corrected experimental data,  $k$  the normalization factor,  $\sum f^2$  the independent scattering from a composition unit and  $g^2(s)$  the sharpening function.

Several functions may be derived depending on the form of  $g^2$  and whether distribution,  $W(r)$ , or density,  $rW(r)$ , functions are considered. Thus for  $g^2 = 1$  electronic distribution or density functions are obtained, whereas with  $g^2 = |\Sigma f|^2$ , atomic functions are obtained. We have illustrated the differences and emphasized the importance of comparing similar functions in another paper<sup>3</sup>. Electronic *RDFs* were originally preferred by Finbak<sup>4</sup> as they tend to minimize termination error, and in any case, the actual sharpening functions employed are usually somewhat arbitrary<sup>5</sup>. For the broad peaks in the *RDF* in which we are interested the 'sharpening' will have little effect, and so the functions used in the rest of this communication are of this form (i.e. electronic).

Figures 1 and 2 show the  $si(s)$  curves and the corresponding electronic *RDFs* for molten polyethylene (PE) and liquid neopentane<sup>6</sup>. Both  $si(s)$  curves contain a prominent peak at  $\sim 1.5 \text{ \AA}^{-1}$  which transforms to a damped oscillation in the *RDF* with a period of about  $5 \text{ \AA}$ . It has been confirmed<sup>7</sup> that the experimental corrections do not affect the damping, by transforming the 'raw data' and avoiding termination effects by using the sampled transform technique.

The  $si(s)$  curve for PE is typical of most non-crystalline polymers in that it contains an intense peak at  $s = 1.0\text{--}1.5 \text{ \AA}^{-1}$ ; however, the scattering function (obtained using electron diffraction<sup>8</sup> for a hydrocarbon gas contains no such intense peak. This absence indicates the intermolecular, or more strictly the interchain, nature of the peak in the scattering function for dense polymer fluids or solids. Non-crystalline polymers, even when molten, have relatively high packing densities ( $\sim 0.6$ ) and so the nearest neighbour distances will have values approaching that of the chain diameter. The sharpness of the distribution of these distances will depend on the regularity of chain shape, local conformation, density and mode of packing. A sharper distribution will give a narrower peak in the scattering function, the width of which is reflected in the corresponding more slowly damped oscillation in the *RDF*.

Unlike polymers, neopentane has roughly spherical molecules and is known to exist as an orientationally disordered plastic crystal below its melting point. Hence the degree of orientational order in the liquid is likely to be small indeed and there is no possibility of parallel chains: yet the peak at  $\sim 1.5 \text{ \AA}^{-1}$  is sharper than for molten PE. We ascribe the greater sharpness of the intermolecular peak in neopentane to the particular regularity of the molecular shape when compared with segments of the PE chain. The curves for neopentane show that local orientational correlation is not a unique requirement for the *RDF* to exhibit a damped oscillation. We will now consider the effect of orientational correlation on *RDFs* by the use of models.

Figure 3 and 4 compare the  $si(s)$  curves and the *RDFs* for two extreme models of non-crystalline polymers with the same packing density. The first consists of short lengths of linear chain segments positioned at the centres of randomly packed spheres, the segments having random orientations. The second consists of long linear chains positioned at the centres of randomly packed parallel cylinders, with no rotational or longitudinal correlations. The calculations have been based on planar zigzags of carbon atoms, although we are not concerned here with the fine detail of the models nor their correspondence to polymer structures, but utilize them as plausible extremes of packing. The  $si(s)$  curves for the two models (Figure 3) are of the same general form. In each case there is a prominent peak at  $\sim 1.5 \text{ \AA}^{-1}$ , which gives corresponding (and similar) damped oscillations in the *RDFs* (Figure 4). Although differences in the magnitude and positions of the interchain components are apparent in these curves, there are no distinct features which would clearly distinguish between the perfectly aligned and the randomly oriented states of the model segments.

The more significant differences in the scattering functions for the two models in Figure 2 occur for scattering

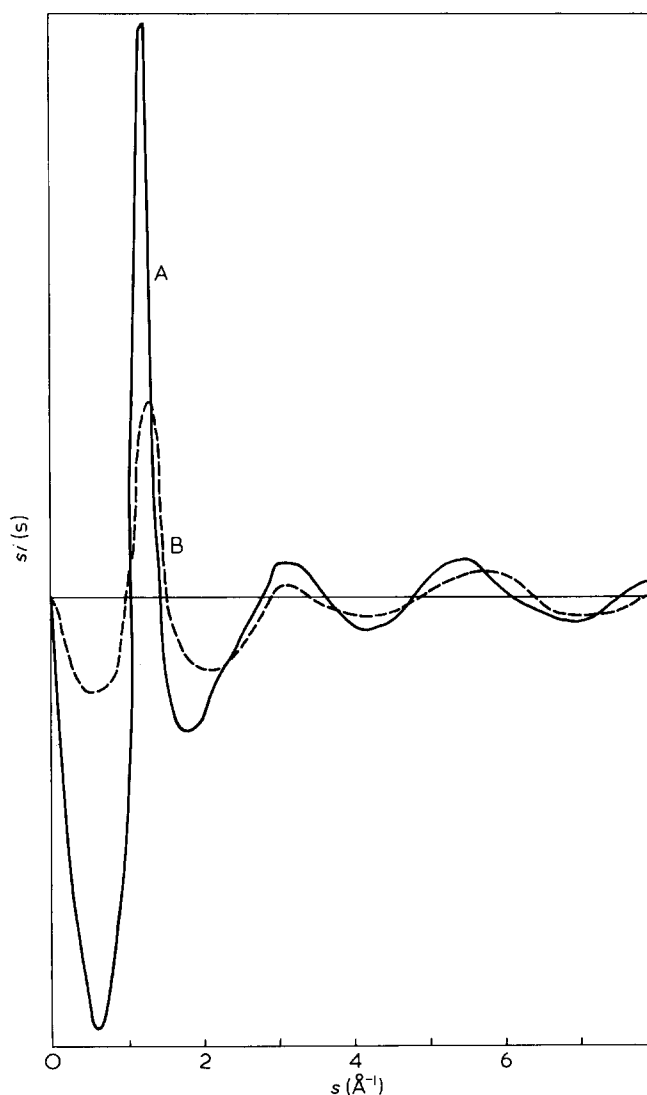


Figure 1  $s$ -weighted intensity function  $si(s)$ . A, Liquid neopentane at  $-17^\circ\text{C}$  calculated from the results of Narten (full line); B, molten polyethylene at  $140^\circ\text{C}$  (broken line)

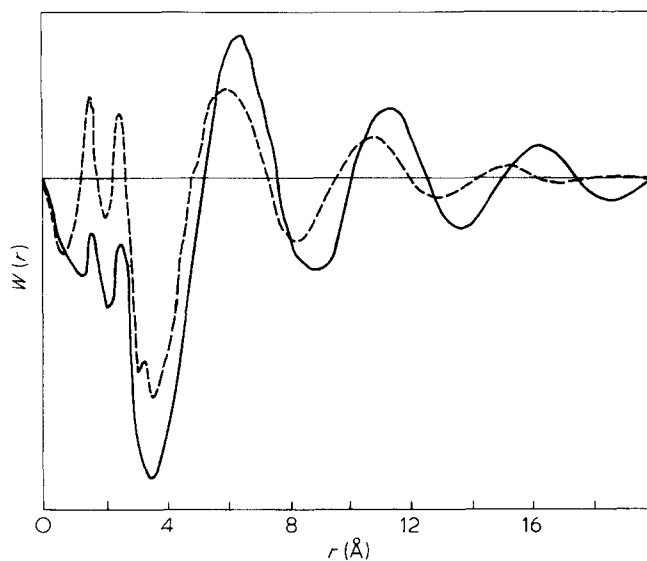


Figure 2 Electronic RDF,  $W(r)$ . A, Liquid neopentane at  $-17^{\circ}\text{C}$  calculated from the results of Narten<sup>6</sup> (full line); B, molten polyethylene at  $140^{\circ}\text{C}$  (broken line)

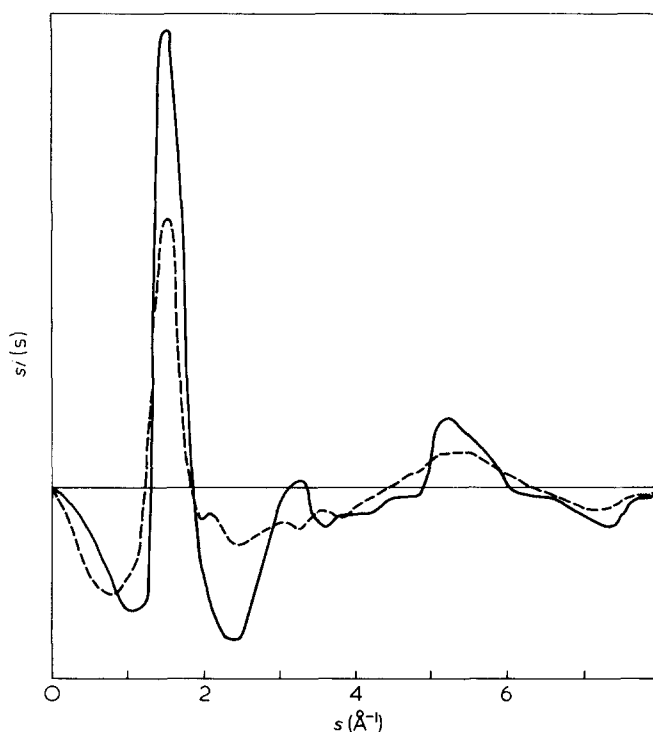


Figure 3 Calculated  $s$ -weighted intensity functions  $si(s)$ . A, Randomly packed parallel carbon planar zigzag chains (full line); B, randomly oriented carbon planar zigzags arranged in the centres of randomly packed spheres (broken line). Both models are enclosed in a sphere of  $25\text{ \AA}$  diameter with a packing density of 0.6. The small-angle scattering due to finite model size has been subtracted

vectors  $> 2.0\text{ \AA}^{-1}$ . This is the part of the scattering which is principally intrachain in origin and so reflects the differing local conformations of the two models. We have described elsewhere<sup>3,9</sup> an approach to the structure determination using wide-angle X-ray scattering which

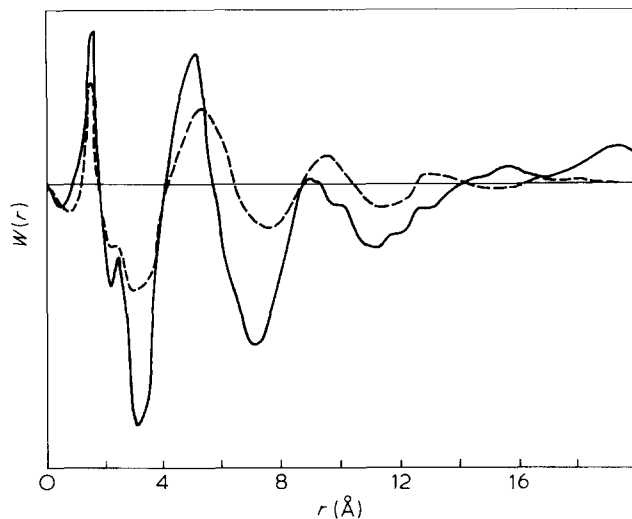


Figure 4 Calculated electronic RDFs  $W(r)$ . A, Randomly packed parallel carbon planar zigzag chains (full line); B, randomly oriented carbon planar zigzags arranged in the centres of randomly packed spheres (broken line). Both models are enclosed in a sphere of  $25\text{ \AA}$  diameter with a packing density of 0.6

considers first the intrachain order before evaluating the interchain packing.

We conclude on the basis of these examples that the rate at which the prominent oscillation in the RDF damps out (or correspondingly the width of the principal broad peak in the scattering function) is not simply related to orientational correlations in non-crystalline polymers, and thus must be interpreted with extreme caution. We also suggest that, in cases where the presence of orientational correlations has been confirmed by other routes, the width and height of the principal scattering peak are more reliable parameters than the subjective measure of the number of broad oscillations in the RDF which has been used previously<sup>10</sup>.

#### Acknowledgements

We are grateful both to Ingrid Voigt-Martin, who while visiting our laboratory encouraged us to consider this issue more fully, and to John Finney of Birkbeck College for the coordinates of the randomly packed spheres. We also thank the Science Research Council for funds.

#### References

- 1 Markova, G. S., Ovchinnikov, Yu. K. and Bokhyan, E. B. *J. Polymer Sci. (Polym. Symp.)* 1973, **42**, 671
- 2 Wang, C. S. and Yeh, G. S. *J. Macromol. Sci. Phys.* 1978, **B15**, 107
- 3 Mitchell, G. R., Lovell, R. and Windle, A. H. to be submitted to *Polymer*
- 4 Finbak, C. *Acta. Chem. Scand.* 1949, **3**, 1279
- 5 Warren, B. E. 'X-ray Diffraction', Addison-Wesley, 1969, p137
- 6 Narten, A. H. *J. Chem. Phys.* 1979, **70**, 299
- 7 Lovell, R., Mitchell, G. R. and Windle, A. H. *Acta. Crystallogr.* 1979, **A35**, 598
- 8 Fischer, E. W. and Dettenmaier, M. *J. Non-Cryst. Solids* 1978, **31**, 181
- 9 Lovell, R., Mitchell, G. R. and Windle, A. H. *Faraday Discuss* 1979, **68**,
- 10 Longman, G. W., Wignall, G. D. and Sheldon, R. P. *Polymer* 1979, **20**, 1063